4394 *Inorg. Chem.* **2010**, *49*, 4394–4404
DOI: 10.1021/ic1004159

Inorganic Chemistry
Article

Extending π-Conjugation of Triarylborons with a 2,2-Bpy Core: Impact of Donor−Acceptor Geometry on Luminescence, Anion Sensing, and Metal Ion Binding

Yi Sun and Suning Wang*

Department of Chemistry, Queen's University, Kingston, Ontario, K7L 3N6, Canada

Received March 2, 2010

Four new 2,2′-bipyridine-based molecules functionalized by either $BMes_2$-phenyl (Mes=mesityl) or NPh_2-phenyl—5,5′-(*p*-$BMes_2$-phenyl)$_2$-2,2′-bpy (5,5′-BP2bpy, **1**), 4,4′-(*p*-$BMes_2$-phenyl)$_2$-2,2′-bpy (4,4′-BP2bpy, **2**), 4-(*p*-$BMes_2$-phenyl)-4′-(*p*-NPh_2-phenyl)-2,2′-bipy (4,4′-BPNPbpy, **4**), and 4,4′-(*p*-NPh_2-phenyl)$_2$-2,2′-bpy (4,4′-NP2bpy, **5**)—have been synthesized. Their complexes with $PtPh_2$ have been synthesized and fully characterized. The electronic and photophysical properties of the new molecules have been examined by electrochemical, absorption, and luminescence spectroscopic analysis and DFT calculations, which show significant differences from those of the related but smaller 2,2′-bpy derivatives functionalized directly by either $BMes_2$ or NPh_2 groups that we reported previously. Molecules **1**, **2**, and **4** and their Pt(II) complexes respond to fluoride ions in both absorption and emission modes. The donor−acceptor molecule **4** and its Pt(II) complex have a distinct fluorescence/phosphorescence turn-on response toward fluoride or cyanide ions. Molecules **1**, **2**, **4**, and **5** also respond to Zn(II) ions in both absorption and emission modes. The diboryl molecules **1** and **2** have a distinct and contrasting fluorescence response toward Zn(II) ion—turn-off for **1** and turn-on for **2**—demonstrating the significant impact of molecular geometry on metal ion binding and fluorescence.

Introduction

π-Conjugated triarylboron compounds have attracted much recent research attention because of their broad applications in optoelectronic devices[1,2] and their ability to function as highly selective sensors[3,4] for certain anions via the disruption of the $p_\pi-\pi$ conjugation around the boron center. A number of research groups have shown recently that the attachment of a metal center to a triarylboron group can have a significant impact on the properties of the molecule.[5,6] We have shown previously that the direct attachment of a boron unit such as $BMes_2$ (Mes = mesityl) to a 2,2-bipy core at the 5 and 5′ positions (e.g., 5,5′-$(BMes_2)_2$-2,2′-bpy, 5,5′-B2bpy) can greatly enhance both electron and fluoride affinity of the boron center.[6a,b] We have further demonstrated that the chelation of such functionalized bipy ligands to a metal ion can not only further increase the electron and anion affinity of the molecule but also introduce distinct colors or bright phosphorescence to the molecule, making the metal complexes attractive sensory materials and potential bifunctional phosphorescent emitters in organic light-emitting diodes. Nonetheless, the $BMes_2$ attachment at the 5 and/or 5′ position of 2,2-bipy does limit the use of the resulting molecules as ligands for binding to metal ions that have a high coordination number due to strong interligand steric interactions. One obvious solution for this problem is to move the $BMes_2$ unit to the 4,4′ position, away from the metal center. Unfortunately our attempts to synthesize molecules such as

*To whom correspondence should be addressed. E-mail: wangs@chem.queensu.ca.

(1) (a) Noda, T.; Shirota, Y. *J. Am. Chem. Soc.* **1998**, *120*, 9714. (b) Shirota, Y. *J. Mater. Chem.* **2005**, *15*, 75. (c) Noda, T.; Ogawa, H.; Shirota, Y. *Adv. Mater.* **1999**, *11*, 283. (d) Shirota, Y.; Kinoshita, M.; Noda, T.; Okumoto, K.; Ohara, T. *J. Am. Chem. Soc.* **2000**, *122*, 1102. (e) Jia, W. L.; Bai, D. R.; McCormick, T.; Liu, Q. D.; Motala, M.; Wang, R.; Seward, C.; Tao, Y.; Wang, S. *Chem.—Eur. J.* **2004**, *10*, 994. (f) Jia, W. L.; Moran, M. J.; Yuan, Y. Y.; Lu, Z. H.; Wang, S. *J. Mater. Chem.* **2005**, *15*, 3326. (g) Jia, W. L.; Feng, X. D.; Bai, D. R.; Lu, Z. H.; Wang, S.; Vamvounis, G. *Chem. Mater.* **2005**, *17*, 164. (h) Li, F. H.; Jia, W. L.; Wang, S.; Zhao, Y. Q.; Lu, Z. H. *J. Appl. Phys.* **2008**, *103*, 034509/1–034509/6. (i) Wakamiya, A.; Mori, K.; Yamaguchi, S. *Angew. Chem., Int. Ed.* **2007**, *46*, 4237.

(2) (a) Collings, J. C.; Poon, S. Y.; Droumaguet, C. L.; Charlot, M.; Katan, C.; Pålsson, L. O.; Beeby, A.; Msely, J. A.; Kaiser, H. M.; Kaufmann, D.; Wong, W. Y.; Blanchard-Desce, M.; Marder, T. B. *Chem.—Eur. J.* **2009**, *15*, 198. (b) Yuan, Z.; Taylor, N. J.; Ramachandran, R.; Marder, T. B. *Appl. Organomet. Chem.* **1996**, *10*, 305. (c) Yuan, Z.; Entwistle, C. D.; Collings, J. C.; Albesa-Jové, D.; Batsanov, A. S.; Howard, J. A. K.; Kaiser, H. M.; Kaufmann, D. E.; Poon, S. −Y.; Wong, W. Y.; Jardin, C.; Fathallah, S.; Boucekkine, A.; Halet, J. F.; Taylor, N. J.; Marder, T. B. *Chem.—Eur. J.* **2006**, *12*, 2758. (d) Entwistle, C. D.; Marder, T. B. *Angew. Chem., Int. Ed.* **2002**, *41*, 2927. (e) Entwistle, C. D.; Marder, T. B. *Chem. Mater.* **2004**, *16*, 4574. (f) Stahl, R.; Lambert, C.; Kaiser, C.; Wortmann, R.; Jakober, R. *Chem.—Eur. J.* **2006**, *12*, 2358. (g) Matsumi, N.; Chujo, Y. *Polym. J.* **2008**, *40*, 77. (h) Lequan, M.; Lequan, R. M.; Ching, K. C. *J. Mater. Chem.* **1991**, *1*, 997. (i) Liu, Z. Q.; Fang, Q.; Cao, D. X.; Wang, D.; Xu, G. B. *Org. Lett.* **2004**, *6*, 2933. (j) Tao, L. M.; Guo, Y. H.; Huang, X. M.; Wang, C. K. *Chem. Phys. Lett.* **2006**, *425*, 10.

 Published on Web 04/23/2010

Chart 1

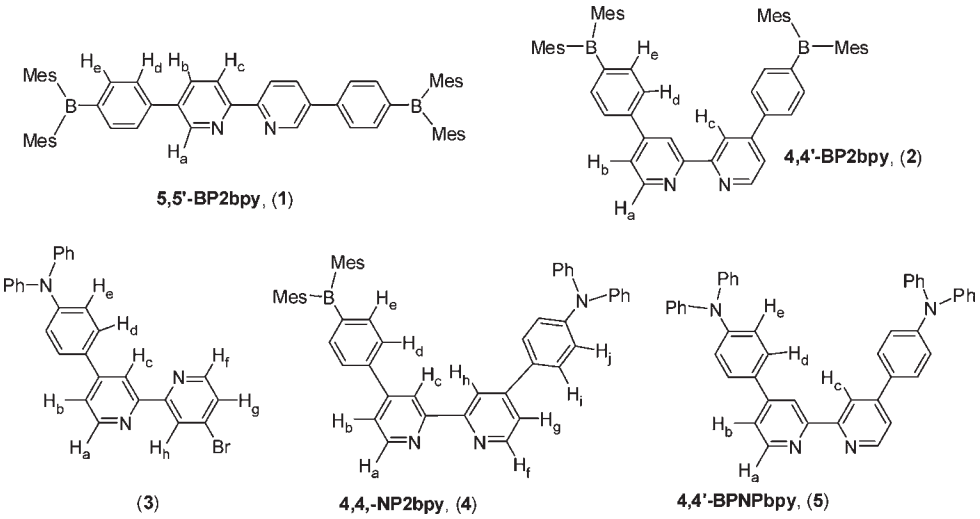

4,4′-($BMes_2$)$_2$-2,2-bpy have not been successful. Our recent efforts have therefore focused on extending the π-conjugation of the $BMes_2$ with the bipy core by inserting a phenyl group so that the bulky $BMes_2$ group is farther away from the metal center, compared to those in 5,5′-B2bpy. We have succeeded in synthesizing 5,5′-(*p*-$BMes_2$-phenyl)$_2$-2,2′-bpy (5,5′-BP2bpy, **1**), 4,4′-(*p*-$BMes_2$-phenyl)$_2$-2,2′-bpy (4,4′-BP2bpy, **2**), the donor−acceptor molecule 4-(*p*-$BMes_2$-phenyl)-4′-(*p*-NPh_2-phenyl)-2,2′-bipy (4,4′-BPNPbpy, **4**), and the donor-only compound 4,4′-(*p*-NPh_2-phenyl)$_2$-2,2′-bpy (4,4′-NP2bpy, **5**) (Chart 1) and the corresponding Pt(II) complexes. We have compared the photophysical and electronic properties of the new ligands and their Pt(II) complexes with those based on 5,5′-B2bpy and 5,5′-BNbpy reported by us earlier,[6a,b] which revealed a significant difference between these two classes of molecules. In addition to Pt(II) ions, we have investigated and compared the interactions of this new group of ligands with Zn(II) ions. Distinct differences have also been observed between 4,4′-BP2bpy and 5,5′-BP2bpy and their complexes. The full account is presented herein.

Experimental Section

All reactions were performed under dry N_2 with standard Schlenk techniques unless otherwise noted. All starting materials were purchased from Aldrich Chemical Co. and used without further purification. THF, toluene, and CH_2Cl_2 were purified using the solvent purification system (Innovation Technologies Co.). Deuterated solvents $CDCl_3$ and CD_2Cl_2 (Cambridge Isotopes) were used as received without further drying. NMR spectra were recorded on a Bruker Avance 400 spectrometer (400.13 MHz for ^{1}H, 100.62 MHz for ^{13}C). UV−vis spectra were recorded on an Ocean Optics ISS-UV−vis spectrophotometer. Cyclic voltammetry was performed using a BAS CV-50W analyzer with a scan rate of 500 mV/s to 4 V/s and a typical concentration of 5 mg of the compound in 3 mL of DMF, at room temperature using 0.10 M NBu_4PF_6 as the supporting electrolyte. The electrolytic cell used was a conventional three-compartment cell, in which a Pt working electrode, a Pt auxiliary electrode, and an Ag/AgCl reference electrode were employed. The ferrocenium/ferrocene couple was used as the internal standard (E_0 = 0.55 V). Elemental analyses were performed at Canadian Microanalytical Service Lto., Delta, British Columbia. 5,5′-Br_2-2,2′-bipy,[7] 4,4′-Br_2-2,2′-bipy,[7] *p*-Br-phenyl-$BMes_2$,[1e] 2-(4-diphenylaminophenyl)-4,4,5,5,-tetramethyl-1,3,2-dioxaborolane,[8] and [$PtPh_2(SMe_2)]_n$ (n = 2 or 3)[9]

(3) (a) Yamaguchi, S.; Shirasaka, T.; Akiyama, S.; Tamao, K. *J. Am. Chem. Soc.* **2002**, *124*, 8816. (b) Yamaguchi, S.; Akiyama, S.; Tamao, K. *J. Am. Chem. Soc.* **2001**, *123*, 11372. (c) Solé, S.; Gabbaï, F. P. *Chem. Commun.* **2004**, 1284. (d) Melaimi, M.; Gabbaï, F. P. *J. Am. Chem. Soc.* **2005**, *127*, 9680. (e) Chiu, C. W.; Gabbaï, F. P. *J. Am. Chem. Soc.* **2006**, *128*, 14248. (f) Hudnall, T. W.; Melaimi, M.; Gabbaï, F. P. *Org. Lett.* **2006**, *8*, 2747. (g) Lee, M. H.; Agou, T.; Kobayashi, J.; Kawashima, T.; Gabbaï, F. P. *Chem. Commun.* **2007**, 1133. (h) Lee, M. H.; Gabbaï, F. P. *Inorg. Chem.* **2007**, *46*, 8132. (i) Hudnall, T. W.; Gabbaï, F. P. *J. Am. Chem. Soc.* **2007**, *129*, 11978. (j) Dorsey, C. L.; Jewula, P.; Hudnall, T. W.; Hoefelmeyer, J. D.; Taylor, T. J.; Honesty, N. R.; Chiu, C.-W.; Schulte, M.; Gabbaï, F. P. *Dalton Trans.* **2008**, 4442. (k) Hudnall, T. W.; Kim, Y.-M.; Bebbington, M. W. P.; Bourissou, D.; Gabbaï, F. P. *J. Am. Chem. Soc.* **2008**, *130*, 10890. (l) Kim, Y.; Gabbai, F. P. *J. Am. Chem. Soc.* **2009**, *131*, 3363. (m) Hudnall, T. W.; Chiu, C.-W.; Gabbai, F. P. *Acc. Chem. Res.* **2009**, *42*, 388.

(4) (a) Sundararaman, A.; Venkatasubbaiah, K.; Victor, M.; Zakharov, L. N.; Rheingold, A. L.; Jäkle, F. *J. Am. Chem. Soc.* **2006**, *128*, 16554. (b) Parab, K.; Venkatasubbaiah, K.; Jäkle, F. *J. Am. Chem. Soc.* **2006**, *128*, 12879. (c) Jäkle, F. *Coord. Chem. Rev.* **2006**, *250*, 1107. (d) Li, H. Y.; Sundararaman, A.; Venkatasubbaiah, K.; Jäkle, F. *J. Am. Chem. Soc.* **2007**, *129*, 5792. (e) Liu, X. Y.; Bai, D. R.; Wang, S. *Angew. Chem., Int. Ed.* **2006**, *45*, 5475. (f) Bai, D. R.; Liu, X. Y.; Wang, S. *Chem.—Eur. J.* **2007**, *13*, 5713. (g) Zhao, S. B.; Wucher, P.; Hudson, Z. M.; McCormick, T. M.; Liu, X. Y.; Wang, S.; Feng, X. D.; Lu, Z. H. *Organometallics* **2008**, *27*, 6446. (h) Zhou, G.; Baumgarten, M.; Müllen, K. *J. Am. Chem. Soc.* **2008**, *130*, 12477. (i) Hudson, Z. M.; Wang, S. *Acc. Chem. Soc.* **2009**, *42*, 1584.

(5) (a) Sakuda, E.; Funahashi, A.; Kitamura, N. *Inorg. Chem.* **2006**, *45*, 10670. (b) Zhou, G. J.; Ho, C. L.; Wong, W. Y.; Wang, Q.; Ma, D. G.; Wang, L. X.; Lin, Z. Y.; Marder, T. B.; Beeby, A. *Adv. Funct. Mater.* **2008**, *18*, 499. (c) You, Y. M.; Park, S. Y. *Adv. Mater.* **2008**, *20*, 3820. (d) Zhao, Q.; Li, F. Y.; Liu, S. J.; Yu, M. X.; Liu, Z. Q.; Yi, T.; Huang, C. H. *Inorg. Chem.* **2008**, *47*, 9256. (e) Venkatasubbaiah, K.; Nowik, I.; Herber, R. H.; Jäkle, F. *Chem. Commun.* **2007**, 2154. (f) Venkatasubbaiah, K.; Pakkirisamy, T.; Lalancette, R. A.; Jäkle, F. *Dalton Trans.* **2008**, 4507. (g) Broomsgrove; Alexander, E. J.; Addy, D. A.; Bresner, C.; Fallis, I. A.; Thompson, A. L.; Aldridge, S. *Chem.—Eur. J.* **2008**, *14*, 7525. (h) Day, J. K.; Bresner, C.; Coombs, N. D.; Fallis, I. A.; Ooi, L. L.; Aldridge, S. *Inorg. Chem.* **2008**, *47*, 793. (i) Lam, S. T.; Zhu, N.; Yam, V. W. W. *Inorg. Chem.* **2009**, *48*, 9664. (j) Wade, C. R.; Gabbai, F. P. *Inorg. Chem.* **2010**, *49*, 714.

(6) (a) Sun, Y.; Ross, N.; Zhao, S. B.; Huszarik, K.; Jia, W. L.; Wang, R. Y.; Wang, S. *J. Am. Chem. Soc.* **2007**, *129*, 7510. (b) Sun, Y.; Wang, S. *Inorg. Chem.* **2009**, *48*, 3755. (c) Zhao, S. B.; McCormick, T.; Wang, S. *Inorg. Chem.* **2007**, *46*, 10965. (d) Hudson, Z. M.; Zhao, S. B.; Wang, S. *Chem.—Eur. J.* **2009**, *15*, 6081. (e) Rao, Y. L.; Wang, S. *Inorg. Chem.* **2009**, *48*, 7698.

(7) (a) Liu, S.-J.; Zhao, Q.; Chen, R.-F.; Deng, Y.; Fan, Q.-L.; Li, F.-Y.; Wang, L.-H.; Huang, C.-H.; Huang, W. *Chem.—Eur. J.* **2006**, *12*, 4351. (b) Nakashima, K.; Shinkai, S. *Chem. Lett.* **1994**, 1267.

(8) Medina, A.; Claessens, C. G.; Rahman, G. M. A.; Lamsabhi, A. M.; Mó, O.; Yáñez, M.; Guldi, D. M.; Torres, T. *Chem. Commun.* **2008**, 1759.

(9) (a) Song, D.; Wang, S. *J. Organomet. Chem.* **2002**, *648*, 302. (b) Scott, J. D.; Puddephatt, R. J. *Organometallics* **1983**, *2*, 1643.

were prepared by modified methods described in the literature.

Synthesis of 5,5′-BP2bpy (1). To a solution of *p*-Br-phenyl-$BMes_2$ (505 mg, 1.25 mmol) in 2 mL of THF was added dropwise *n*-BuLi (0.86 mL, 1.30 mmol) at −78 °C, and the reaction mixture was stirred at this temperature for 1 h. Anhydrous $ZnCl_2$ (255 mg, 1.85 mmol) was then added, and the reaction mixture was allowed to warm to room temperature and stirred for an additional 2 h. A THF (2 mL) solution of Pd-$(PPh_3)_4$ (5 mol %, 145 mg) and 5,5′-Br_2-2,2′-bipy (157 mg, 0.50 mmol) was then added. After the mixture was stirred at 55 °C for 48 h, a saturated aqueous NH_4Cl solution was added and the product was extracted with CH_2Cl_2. The organic portions were combined and dried with $MgSO_4$. After removing the solvent, the residue was separated by column chromatography in silica gel, eluting with 10% (v/v) ethyl acetate/hexane, to give 262 mg (65%) of **2** as white solids. ^{1}H NMR (400 MHz, CD_2Cl_2): 8.99 (d, J = 1.5 Hz, 2H, H_a), 8.56 (d, J = 6.3 Hz, 2H, H_b), 8.12 (dd, J = 1.5 Hz, J = 6.3 Hz, 2H, H_c), 7.70 (d, J = 6.3 Hz, 4H, H_d), 7.61 (d, J = 6.3 Hz, 4H, H_e), 6.86 (s, 8H, *H* of Mes), 2.32 (s, 12H, CH_3 of Mes), 2.04 (s, 24H, CH_3 of Mes). ^{13}C NMR (100 MHz, CD_2Cl_2): 154.6, 148.2, 142.9, 141.1, 139.3, 137.5, 135.6, 128.6, 126.8, 121.2, 112.9, 111.0 (aryl *C*), 23.6, 21.3 (*C*H_3 of Mes). HRMS: calcd for $C_{58}H_{59}B_2N_2$, $[M + 1]^+$ 805.4864; found 805.4874.

4,4′-BP2bpy (2). This compound was prepared as white solids from 4,4′-Br_2-2,2′-bipy (157 mg, 0.50 mmol) using the same procedure as described for **1**: yield 242 mg (60%). ^{1}H NMR (400 MHz, CD_2Cl_2): 8.80 (d, J = 1.5 Hz, 2H, H_a), 8.73 (d, J = 5.1 Hz, 2H, H_c), 7.78 (d, J = 8.1 Hz, 4H, H_d), 7.62 (d, J = 8.1 Hz, 4H, H_e), 7.71 (d, J = 5.1 Hz, 2H, H_b), 6.86 (s, 8H, *H* of Mes), 2.32 (s, 12H, CH_3 of Mes), 2.02 (s, 24H, CH_3 of Mes). ^{13}C NMR (100 MHz, CD_2Cl_2): 153.9, 149.7, 148.9, 142.9, 141.8, 141.2, 139.7, 139.2, 137.3, 133.5, 132.4, 129.0, 128.9, 128.7, 127.4, 125.5, 120.4 (aryl *C*), 23.6, 21.3 (*C*H_3 of Mes). HRMS: calcd for $C_{58}H_{59}B_2N_2$, $[M + 1]^+$ 805.4864; found 805.4866.

4-Br-4′-(*p*-NPh_2-phenyl)-2,2′-bpy (3) and 4,4′-NP2bpy (5). The mixture of 4,4′-Br_2-2,2′-bipy (471 mg, 0.50 mmol), Pd-$(PPh_3)_4$ (45 mg g, 0.04 mmol), and toluene (20 mL) was stirred for 10 min. 2-(4-Diphenylaminophenyl)-4,4,5,5,-tetramethyl-1,3,2-dioxaborolane (220 mg, 0.6 mmol) in 10 mL of EtOH and NaOH (800 mg) in 10 mL of H_2O were subsequently added. The mixture was stirred and heated at reflux for 40 h. After cooling to room temperature, the water layer was separated and extracted with CH_2Cl_2 (3 × 30 mL). The combined organic layers were dried over $MgSO_4$, and the solvents were evaporated under reduced pressure. Purification of the crude product by column chromatography (ethyl acetate/hexane, 1:5) afforded **3** as a yellow solid in 32% yield and **4** as a yellow solid in 23% yield. For **3**, ^{1}H NMR (400 MHz, $CDCl_3$): 8.67 (m, 2H, H_a+H_c), 8.63 (s, 1H, H_f), 8.49 (d, J = 4.8 Hz, 1H, H_h), 7.64 (d, J = 8.1 Hz, 2H, H_d), 7.52 (dd, J = 1.2 Hz, J = 4.8 Hz, 1H, H_b), 7.49 (dd, J = 1.2 Hz, J = 4.8 Hz, 1H, H_g), 7.30 (t, J = 7.6 Hz, 4H, *ph*), 7.15 (m, 6H, H_e + *ph*), 7.08 (t, J = 7.6 Hz, 2H, *ph*). ^{13}C NMR (100 MHz, CD_2Cl_2): 157.8, 155.5, 150.1, 150.0, 149.3, 149.1, 147.6, 134.3, 131.3, 129.8, 128.2, 127.2, 125.3, 125.0, 123.9, 123.2, 121.7, 118.9. HRMS: calcd for $C_{28}H_{20}BrN_3$, $[M]^+$ 477.0845; found 477.0841. For **5**, ^{1}H NMR (400 MHz, $CDCl_3$): 8.69 (d, 2H, H_c), 8.68 (s, 2H, H_a), 7.66 (d, J = 6.8 Hz, 4H, H_d), 7.51 (dd, J = 1.2 Hz, J = 4.8 Hz, 2H, H_b), 7.30 (t, J = 7.6 Hz, 8H, *ph*), 7.15 (m, 12H, H_e + *ph*), 7.08 (t, J = 7.6 Hz, 4H, *ph*). ^{13}C NMR (100 MHz, CD_2Cl_2): 157.1, 149.3, 149.1, 147.7, 147.0, 131.8, 129.8, 128.3, 125.4, 125.2, 123.8, 123.5, 123.4, 121.3, 120.6, 119.0. HRMS: calcd for $C_{46}H_{35}N_4$, $[M + 1]^+$ 643.2861; found 643.2883.

4,4′-BPNPbpy (4). To a solution of *p*-Br-phenyl-$BMes_2$ (207 mg, 0.51 mmol) in 2 mL of THF was added dropwise *n*-BuLi (0.35 mL, 0.57 mmol) at −78 °C, and the reaction mixture was stirred for 1 h. After the addition of anhydrous $ZnCl_2$ (83 mg, 0.56 mmol), the reaction mixture was allowed to warm to room temperature and stirred for an additional 2 h before a THF (2 mL) solution of $Pd(PPh_3)_4$ (5 mol %, 20 mg) and **3** (162 mg, 0.34 mmol) was added. After the mixture was stirred at 55 °C for 48 h, a saturated aqueous NH_4Cl solution was added and the product was extracted with CH_2Cl_2. All organic portions were combined and dried with $MgSO_4$. After removing the solvent, the residue was purified by column chromatography in silica gel, eluting with 20% (v/v) ethyl acetate/CH_2Cl_2 to give 130 mg (53%) of **4** as a yellow solid. ^{1}H NMR (400 MHz, CD_2Cl_2): 8.78 (d, J = 1.2 Hz, 1H, H_a), 8.74 (d, J = 1.2 Hz, 1H, H_f), 8.73 (d, J = 5.2 Hz, 1H, H_h), 8.67 (d, J = 5.2 Hz, 1H, H_c), 7.78 (d, J = 8.4 Hz, 2H, H_e), 7.69 (d, J = 8.4 Hz, 2H, H_d), 7.62 (d, J = 8.4 Hz, 2H, H_i), 7.61 (dd, J = 2.0 Hz, J = 5.2 Hz, 1H, H_b), 7.54 (dd, J = 2.0 Hz, J = 5.2 Hz, 1H, H_g), 7.31 (t, J = 7.6 Hz, 4H, *ph*), 7.15 (m, 6H, H_j + *ph*), 7.09 (t, J = 7.6 Hz, 2H, *ph*), 6.86 (s, 4H, *H* of Mes), 2.32 (s, 6H, CH_3 of Mes), 2.03 (s, 12H, CH_3 of Mes). ^{13}C NMR (100 MHz, CD_2Cl_2): 157.1, 156.7, 150.0, 149.3, 149.1, 148.7, 147.6, 146.9, 141.9, 141.8, 141.1, 139.2, 137.2, 131.5, 129.7, 128.5, 128.1, 127.0, 125.3, 123.9, 123.2, 121.9, 121.2, 119.3, 119.2, 118.4, 118.3 (aryl *C*), 23.5, 21.3 (*C* of Mes). HRMS: calcd for $C_{52}H_{47}BN_3$, $[M+1]^+$ 724.3872; found 724.3862.

Pt(5,5′-BP2bpy)Ph_2 (1a). Ligand **1** (80 mg, 0.10 mmol) and $[PtPh_2(\mu\text{-}SMe_2)]_n$ (n = 2 or 3) (41 mg, 0.10 mmol) were mixed in 20 mL of CH_2Cl_2 and stirred for 12 h under nitrogen at room temperature. After removing the solvent, the red residue was washed by Et_2O and dried under vacuum to afford **1a** in 82% yield. ^{1}H NMR (400 MHz, CD_2Cl_2): 8.88 (d, J = 1.6 Hz, 2H, H_a), 8.38 (dd, J = 1.2 Hz, J = 6.8 Hz, 2H, H_b), 8.17 (d, J = 6.8 Hz, 2H, H_c), 7.56 (d, J = 6.4 Hz, 4H, H_e), 7.51 (d, satellite, J = 5.2 Hz, J_{Pt-H} = 64 Hz, 4H, Pt-*Ph*), 7.56 (d, J = 6.4 Hz, 4H, H_d), 7.02 (t, J = 6.0 Hz, 4H, Pt-*Ph*), 6.87 (m, 2H, Pt-*Ph*), 6.85 (s, 8H, *H* of Mes), 2.32 (s, 12H, CH_3 of Mes), 1.99 (s, 24H, CH_3 of Mes). ^{13}C NMR (100 MHz, CD_2Cl_2): 154.9, 148.6, 141.9, 141.2, 139.5, 139.1, 138.6, 138.5, 137.5, 135.4, 132.4, 132.3, 128.9, 128.8, 128.6, 127.4, 126.5, 122.8, 122.4 (aryl *C*), 23.6, 21.3 (*C*H_3 of Mes). Anal. Calcd for $C_{70}H_{68}B_2N_2Pt$: C, 72.86; H, 5.94; N, 2.43. Found: C, 72.96; H, 5.80; N, 2.25.

Pt(4,4′-BP2bpy)Ph_2 (2a). Ligand **2** (80 mg, 0.10 mmol) and $[PtPh_2(\mu\text{-}SMe_2)]_n$ (n = 2 or 3) (41 mg, 0.10 mmol) were mixed in 20 mL of CH_2Cl_2 and stirred for 12 h under nitrogen at room temperature. After removing the solvent, the red residue was washed by Et_2O and dried under vacuum to afford **2a** in 75% yield. ^{1}H NMR (400 MHz, CD_2Cl_2): 8.56 (d, J = 5.6 Hz, 2H, H_a), 8.41 (s, 2H, H_c), 7.74 (d, J = 8.4 Hz, H_e), 7.66 (dd, J = 1.2 Hz, J = 5.6 Hz, 2H, H_b), 7.63 (d, J = 8.4 Hz, 2H, H_d), 7.47 (d, satellite, J = 6.8 Hz, J_{Pt-H} = 64 Hz, 4H, Pt-*Ph*), 7.01 (t, J = 7.6 Hz, 4H, Pt-*Ph*), 6.87 (m, 2H, Pt-*Ph*), 6.86 (s, 8H, *H* of Mes), 2.32 (s, 12H, CH_3 of Mes), 2.00 (s, 24H, CH_3 of Mes). ^{13}C NMR (100 MHz, CD_2Cl_2): 156.9, 150.4, 150.0, 146.5, 141.8, 141.2, 140.1, 139.6, 138.6, 137.3, 128.7, 127.4, 127.0, 125.4, 122.1, 120.8 (aryl *C*), 23.6, 21.3 (*C*H_3 of Mes). Anal. Calcd for $C_{70}H_{68}B_2N_2Pt$: C, 72.86; H, 5.94; N, 2.43. Found: C, 72.51; H, 5.83; N, 2.39.

Pt(4,4′-BPNPbpy)Ph_2 (4a). Ligand **4** (72 mg, 0.10 mmol) and $[PtPh_2(\mu\text{-}SMe_2)]_n$ (n = 2 or 3) (41 mg, 0.10 mmol) were mixed in 20 mL of CH_2Cl_2 and stirred for 12 h under nitrogen at room temperature. After the removal of the solvent, the red residue was washed by Et_2O (10 mL) and dried under vacuum to afford **4a** in 71% yield. ^{1}H NMR (400 MHz, CD_2Cl_2): 8.54 (d, J = 5.6 Hz, 2H, H_a), 8.45 (d, J = 5.6 Hz, 2H, H_f), 8.38 (s, 2H, H_c), 8.33 (s, 2H, H_h), 7.74 (d, J = 8.4 Hz, H_e), 7.64 (m, 5H, H_d + H_i + H_g), 7.57 (dd, J = 1.2 Hz, J = 6.0 Hz, 1H, H_b), 7.47 (m, 4H, Pt-*Ph*), 7.33 (t, J = 7.2 Hz, 4H, N-*Ph*), 7.15 (m, 6H, H_j + N-*Ph*), 7.00 (m, 6H, N-*Ph* + Pt-*Ph*), 6.88 (m, 2H, Pt-*Ph*), 6.86 (s, 4H, *H* of Mes), 2.31 (s, 6H, CH_3 of Mes), 2.01 (s, 12H, CH_3 of Mes). ^{13}C NMR (100 MHz, CD_2Cl_2): 156.1, 154.1, 151.8, 150.4, 150.2, 149.9, 147.3, 145.2, 141.2, 140.1, 139.5, 138.7, 137.3, 132.5, 129.9, 128.7, 128.1, 127.3, 125.8, 125.1, 124.6, 122.4, 120.8 (aryl *C*), 23.6, 21.3 (*C*H_3 of Mes). Anal. Calcd for $C_{64}H_{56}BN_3Pt$: C, 71.64; H, 5.26; N, 3.92. Found: C, 71.91; H, 5.42; N, 4.30.

Scheme 1

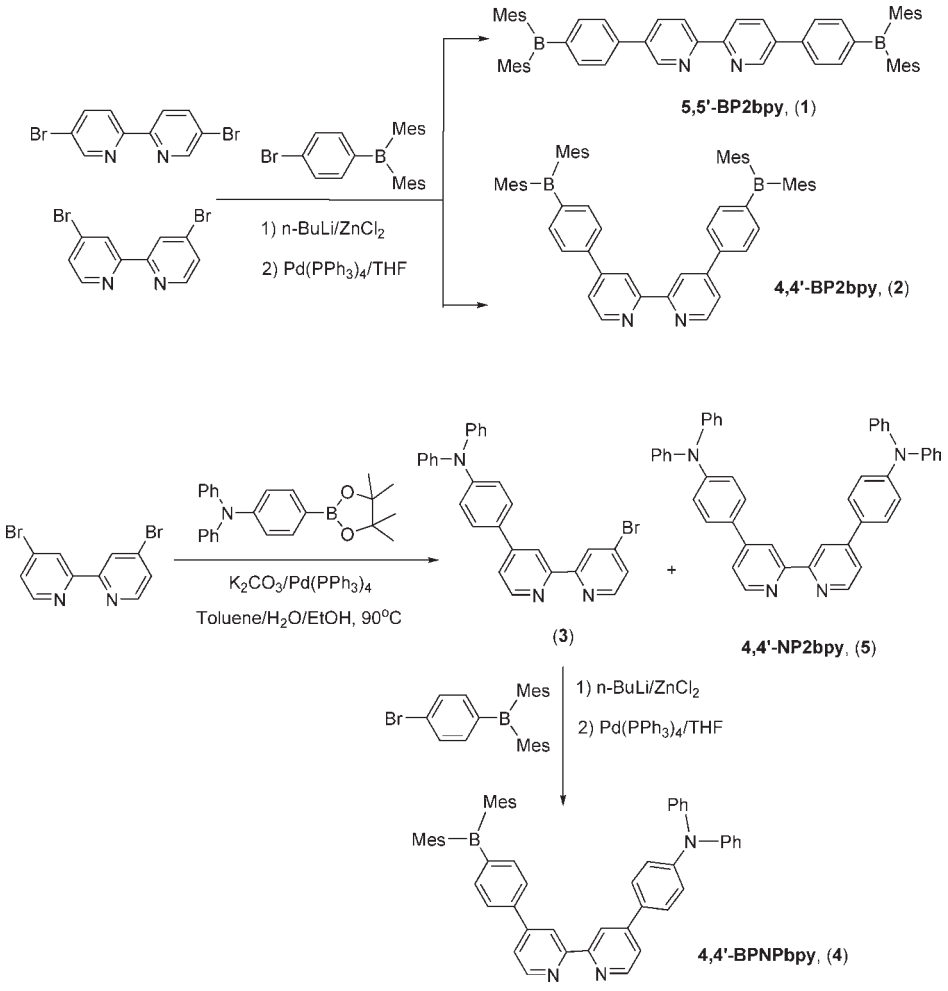

Pt(4,4′-NP2bpy)Ph$_2$ (5a). Ligand **5** (64 mg, 0.10 mmol) and $[PtPh_2(\mu\text{-}SMe_2)]_n$ ($n = 2$ or 3) (41 mg, 0.10 mmol) were mixed in 20 mL of CH_2Cl_2 and stirred for 12 h under nitrogen at room temperature. After the removal of the solvent, the red residue was washed by Et_2O (10 mL) and dried under vacuum to afford **5a** in 65% yield. ^{1}H NMR (400 MHz, CD_2Cl_2): 8.43 (d, $J = 5.6$ Hz, 2H, H_a), 8.30 (s, 2H, H_c), 7.63 (d, $J = 8.8$ Hz, 4H, H_d), 7.54 (d, $J = 5.6$ Hz, 2H, H_b), 7.47 (d, $J = 5.2$ Hz, 4H, Pt-*Ph*), 7.33 (t, $J = 7.6$ Hz, 8H, N-*Ph*), 7.15 (m, 12H, N-*Ph* + H_e), 7.01 (m, 8H, N-*Ph* + Pt-*Ph*), 6.87 (m, 2H, Pt-*Ph*). ^{13}C NMR (100 MHz, CD_2Cl_2): 156.2, 149.8, 149.5, 148.8, 146.6, 146.3, 138.1, 129.3, 128.7, 127.5, 126.7, 125.4, 125.2, 123.9, 121.8, 121.3, 118.9 (aryl *C*). Anal. Calcd for $C_{58}H_{44}N_4Pt$: C, 70.22; H, 4.47; N, 5.65. Found: C, 70.55; H, 4.64; N, 5.32.

[Zn(4,4′-BP2bpy)$_2$][ClO$_4$]$_2$ (2b). Ligand **2** (80 mg, 0.10 mmol) and $Zn(ClO_4)_2$ (18.6 mg, 0.05 mmol) were mixed in 20 mL of CH_2Cl_2 and stirred for 2 h at room temperature. After removal of solvent, the residue was washed by diethyl ether (10 mL) and dried under vacuum to afford **2b** in 82% yield. ^{1}H NMR (400 MHz, CD_2Cl_2): 8.70 (m, 8H, H_a+H_c), 7.98 (d, $J = 6.0$ Hz, 4H, H_b), 7.82 (d, $J = 8.0$ Hz, 8H, H_e), 7.68 (d, $J = 8.0$ Hz, 8H, H_d), 6.86 (s, 16H, *H* of Mes), 2.32 (s, 24H, CH_3 of Mes), 2.02 (s, 48H, CH_3 of Mes). ^{13}C NMR (100 MHz, CD_2Cl_2): 155.9, 151.4, 150.5, 146.1, 141.5, 141.2, 140.6, 139.3, 138.7, 136.3, 128.2, 127.2, 126.8, 124.4, 122.5, 120.4 (aryl *C*), 23.6, 21.3 (*C*H$_3$ of Mes). HRMS: calcd for $C_{116}H_{116}B_4ClN_4O_4Zn$, $[M - ClO_4]^+$ 1771.8348; found 1771.8402.

Results and Discussions

Syntheses and Structures. The new bpy derivatives 5,5′-BP2bpy (**1**) and 4,4′-BP2bpy (**2**) were synthesized by the reaction of *p*-Br-phenyl-BMes$_2$ with 5,5′-Br$_2$-2,2′-bpy or 4,4′-Br$_2$-2,2′-bpy using a Negishi coupling procedure[10] with $Pd(PPh_3)_4$ as the catalysts (Scheme 1). The donor-only molecule 4,4′-NP2bpy (**5**) ligand was obtained as a byproduct in 23% yield from the Suzuki−Miyaura coupling reaction[11] for the synthesis of **3**, a precursor for the synthesis of the donor−acceptor molecule 4,4′-BPNPbpy (**4**). Negishi coupling of **3** with *p*-Br-phenyl-BMes$_2$ produced compound **4** in 53% yield (Scheme 1). Compounds **1** and **2** are white solids, while compounds **4** and **5** are both yellow solids. The PtPh$_2$ complexes Pt(5,5′-BP2bpy)Ph$_2$ (**1a**), Pt(4,4′-BP2bpy)Ph$_2$ (**2a**), Pt(4,4′-BPNPbpy)Ph$_2$ (**4a**), and Pt(4,4′-NP2bpy)Ph$_2$ (**5a**) were obtained by the reaction of the chelate ligands with $[PtPh_2(SMe_2)]_n$ in high yields. The structures of all Pt(II) complexes are shown in Chart 2. They all have an orange color and are air-stable in both solution and the solid state. The ligands and their Pt(II) complexes have been fully characterized by NMR spectroscopy and HR-MS or element analyses. The crystal structure of **2** was determined by X-ray diffraction and is shown in Figure 1. One half of molecule **2** is related to the other half by an inversion

(10) Kiehne, U.; Bunzen, J.; Staats, H.; Lützen, A. *Synthesis* **2007**, 1061.
(11) (a) Kotha, S.; Lahiri, K.; Kashinath, D. *Tetrahedron* **2002**, *58*, 9633. (b) Suzuki, A. *Acc. Chem. Res.* **1982**, *15*, 178. (c) Miyaura, N.; Suzuki, A. *Chem. Rev.* **1995**, *95*, 2457.

Chart 2

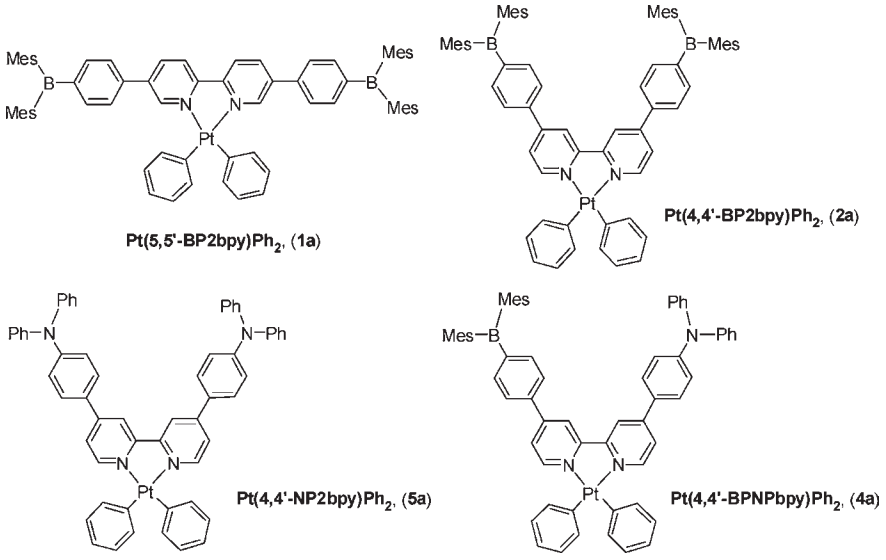

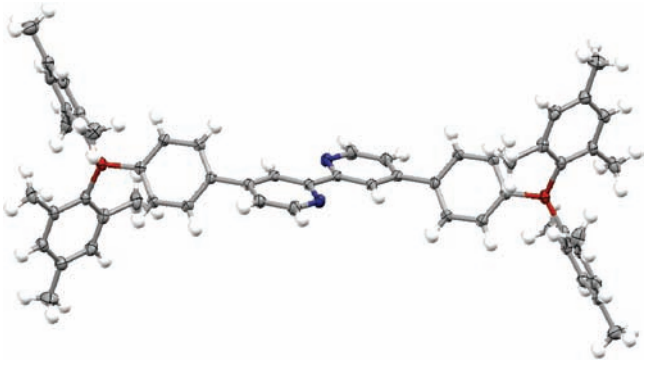

Figure 1. Diagram showing the structure of ligand **2** with 35% thermal ellipsoids.

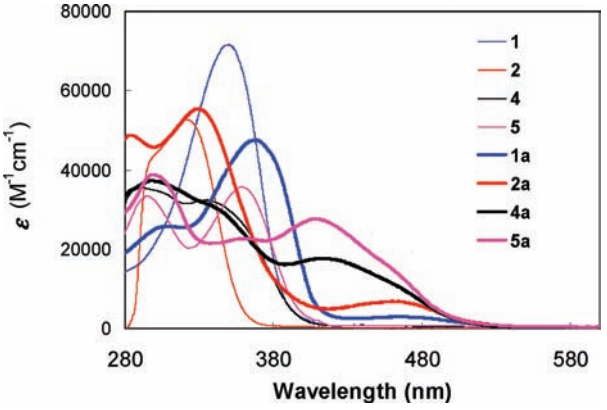

Figure 2. UV−vis absorption spectra of free ligands (**1**, **2**, **4**, and **5**) and their Pt(II) complexes (**1a**, **2a**, **4a**, and **5a**) recorded in CH_2Cl_2.

center. The central bpy unit is coplanar. The phenyl ring has a dihedral angle of 53.8° with the bpy ring (see Supporting Information (SI) for details). None of the Pt(II) complexes produced single crystals suitable for X-ray diffraction analysis.

Absorption Spectra. In CH_2Cl_2, the free ligands show a strong absorption between 290 and 360 nm. Among the 4,4′-functionalized bpy ligands, the λ_{max} of the low-energy absorption band follows the order 4,4′-BP2bpy (**2**) (321 nm) < 4,4′-BPNPbpy (**4**) (337 nm) < 4,4′-NP2bpy (**5**) (358 nm). As shown in Figure 2 and Table 1, the absorption energy of **1** is about 30 nm lower than that of **2**, attributable to the more effective π-conjugation in 5,5′-BP2bpy. The corresponding Pt(II) complexes all have a broad and weak absorption band, characteristic of metal-to-ligand charge-transfer (MLCT) transitions. The MLCT energy for the 4,4′-substituted bpy complexes follows the order **5a** < **4a** (418 nm) < **2a** (460 nm), in agreement with the electron-accepting nature of the boron center that lowers the MLCT energy in **2a** and **4a**. The MLCT energy (468 nm) of **1a** is much higher than that (525 nm) of Pt(5,5′-B2bpy)Ph_2, where two $BMes_2$ are directly attached to the bpy group,[6a,b] indicating that the impact of the $BMes_2$ as an electron-accepting group decreases significantly as its distance from the Pt(II) center increases.

Reduction Potentials. The reduction potential of the free ligands and the corresponding Pt(II) complexes were recorded by cyclic voltammetry and are shown in Figure 3. Ligands **1**, **2**, and **4** all have two reversible reduction peaks with a similar first reduction peak (−2.04 V, vs $FeCp_2^{0/+}$), which is attributed to the reduction of the boron center and the conjugated biphenylbpy linker. In contrast, ligand **5** has only one reversible reduction at −2.47 V (vs $FeCp_2^{0/+}$), much more negative than the first reduction potential of other ligands, supporting that the boron center enhances the electron-accepting ability in compounds **1**, **2**, and **4**. The first reduction peaks for the four Pt(II) complexes were observed at −1.61 V (**1a**), −1.73 V (**2a**), −1.78 V (**4a**), and −1.89 V (**5a**), respectively, which are all more positive than that of the corresponding free ligand, in agreement with the trend observed for the previously reported $PtPh_2$ complexes[6a,b] of 5,5′-B2bpy, 5,5′-BNbpy, and 5,5′-N2bpy. However, compared to that of Pt(5,5′-B2bpy)Ph_2 (−1.34 V), the reduction potential of **1a** and **2a** is much more negative, attributed to the diminished impact of the $BMes_2$ group on the electron-accepting ability of the molecule in **1a** and **2a** due to the longer separation distance from the chelate site. Using the CV and UV−vis data, the HOMO and

Table 1. Absorption and Luminescence Data

compound	UV−vis, nm (ε, M^{-1} cm^{-1})	λ_{em}, nm/τ,[a] μs CH_2Cl_2, rt	λ_{em}, nm/τ, ms, CH_2Cl_2, 77 K	Φ,[b] CH_2Cl_2
1	350 (71 589)	390/7.7(2)	549/0.5(1)	0.35
2	321 (52 745)	415/5.8(1)	466, 500/1.5(3), 1.1(2)	0.076
4	337 (32 253)	459/6.6(2)	503, 531/0.8(1), 0.9(1)	0.14
5	358 (35 646)	455/7.0(1)	507/3.0(1)	0.52
1a	369 (47 451), 468 (2929)	N/A	547/0.010(1)	N/A
2a	330 (55 328), 460 (6842)	N/A	540/0.009(1)	N/A
4a	345 (30 168), 418 (17 564)	577/8.5(1)	537/0.022(1)	0.0017
5a	360 (35 573), 409 (27 579)	577/7.6(1)	545/0.027(1)	0.0066

[a] Decay lifetime at rt for the Pt(II) complexes was measured under N_2. [b] The quantum efficiency for the free ligands was obtained under air using 9,10-diphenylanthracene as the standard. For the Pt(II) complexes, the quantum efficiency was measured under N_2 using $Ir(ppy)_3$ as the standard (Φ = 0.40).[12] The quantum efficiencies of complexes **4a** and **5a** versus $Ir(ppy)_3$ under air are 0.0014 and 0.0056, respectively (Φ = 0.0068 for $Ir(ppy)_3$ under air, assuming Φ = 0.40 for $Ir(ppy)_3$ under N_2).

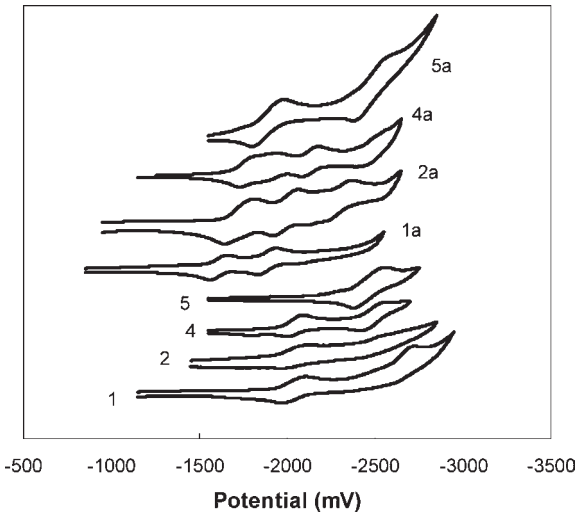

Figure 3. CV diagrams for all ligands (**1**, **2**, **4**, and **5**) and complexes (**1a**, **2a**, **4a**, and **5a**) recorded in DMF. The potential is relative to that of $FeCp_2^{+/0}$.

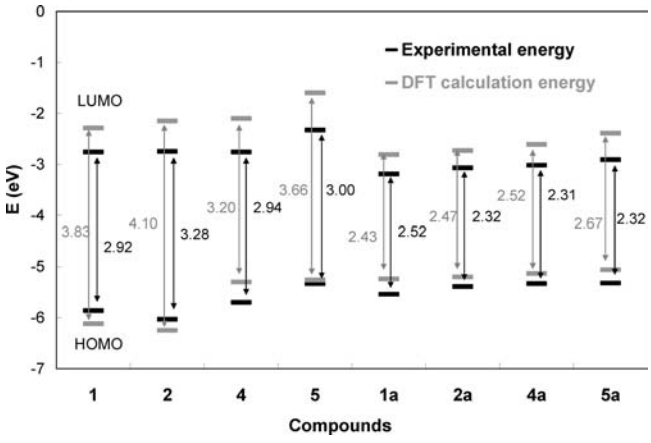

Figure 4. HOMO and LUMO energy levels of the free ligands **1**, **2**, **4**, and **5** and the Pt(II) complexes **1a**, **2a**, **4a**, and **5a**.

LUMO energies of the ligands and their complexes were estimated and are shown in Figure 4 (see also Table 3 in the SI). The data show consistently the stabilization of the LUMO level of free ligands by metal chelation.

DFT Calculations. Molecular orbital calculations were performed for all compounds using the Gaussian suite of programs (Gaussian 03)[13] and the basis set B3LYP-6-311G(d). The calculated HOMO and LUMO energy level and the energy gaps for the ligands and the complexes are shown in Figure 4. The calculated HOMO−LUMO trend is consistent with that observed experimentally. The HOMO and LUMO orbitals of the free ligands and all metal complexes are shown in Figure 5a and b, respectively.

The HOMO level for **1** is a π orbital dominated by the bpy unit, while the HOMO level of **2** has contributions almost exclusively from the mesityls. The LUMO levels of **1** and **2** are π^* orbitals dominated by the two boron atoms and the bpy units. For **5**, the HOMO level is a π orbital involving the two NPh_2 groups, while the LUMO level is a π^* orbital dominated by a bpy unit. Hence, the lowest electronic transition in these molecules can be considered as a π to π^* transition (**1**) and charge-transfer transition (mesityl to B in **2**, N to bpy in **5**), respectively. The HOMO level of **4** involves the NPh_2 group, while the LUMO is dominated by the phenyl-$BMes_2$ group, supporting that the lowest electronic transition of this molecule is charge transfer from the amino group to the B center, mediated by the bpy unit. For the Pt(II) complexes, the HOMO level consists of π orbitals of the two phenyl ligands and the d orbital of Pt(II) center, while the LUMO level involves π^* orbitals of the chelate ligand with some d orbital contributions of the Pt(II) center. The lowest electronic transition of all Pt complexes can be therefore considered as charge transfer from $PtPh_2$ to the π^* orbital of the ligands.

Luminescence. All four free ligands are blue fluorescent in solution, the solid state with **5** being the brightest (ϕ = 0.52). Consistent with the lowest electronic transition being charge transfer, the emission band of **2**, **4**, and **5** shows dependence on the solvent polarity (e.g., ~50 nm red shift from toluene to CH_3CN for **2**, 100 nm for **4** and **5**, see SI). In contrast, the emission of **1** has little dependence on solvent polarity. The Pt(4,4′-BPNPbpy)Ph_2 (**4a**) and Pt(4,4′-NP2bpy)Ph_2 (**5a**) complexes display ambient-temperature phosphorescence with λ_{max} = 577 nm, τ = 8.5(1) μs and λ_{max} = 577 nm, τ = 7.6(1) μs, respectively, in CH_2Cl_2 (Figure 6), which is most likely from a ligand-centered triplet state, due to the similarity of the emission peak profile with the phosphorescence emission peak of

(12) (a) King, K. A.; Spellane, P. J.; Watts, R. J. *J. Am. Chem. Soc.* **1985**, *107*, 1431. (b) Lamansky, S.; Djurovich, P.; Murphy, D.; Abdel-Razzaq, F.; Kwong, R.; Tsyba, I.; Bortz, M.; Mui, B.; Bau, R.; Thompson, M. E. *Inorg. Chem.* **2001**, *40*, 1704.

(13) Frisch, M. J.; et al. *Gaussian 03, Revision C.02*; Gaussian, Inc.: Wallingford, CT, 2004.

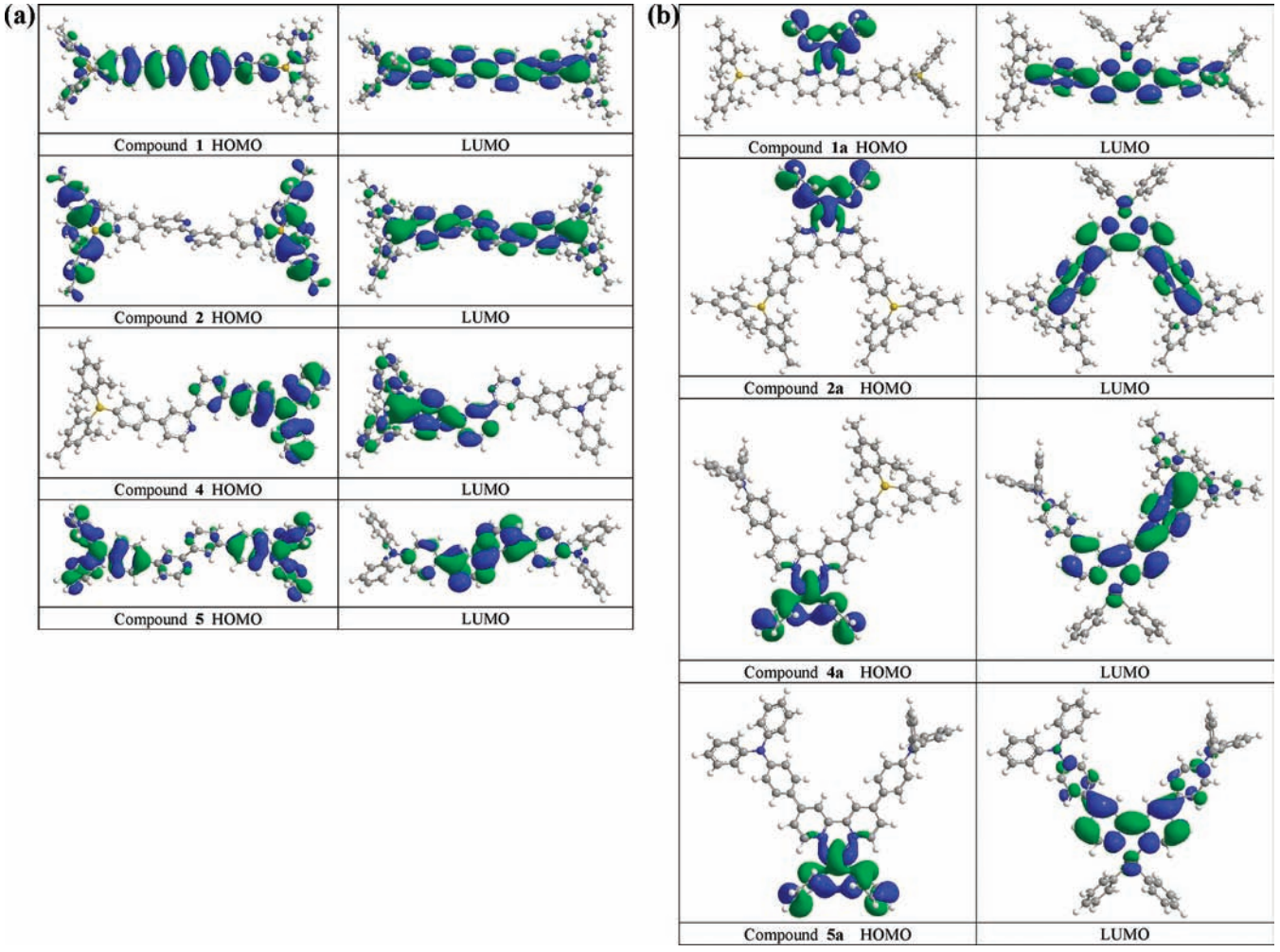

Figure 5. (a) HOMO and LUMO diagrams of ligands **1**, **2**, **4**, and **5**. (b) HOMO and LUMO diagrams of the Pt(II) complexes **1a**, **2a**, **4a**, and **5a**.

the corresponding free ligand at 77 K (see SI). The phosphorescent decay lifetimes of these two Pt(II) complexes at 77K are all much shorter than those of the free ligands, consistent with the heavy atom effects in the complexes. Although under nitrogen the emission quantum efficiency of **4a** and **5a** is much lower than that of $Ir(ppy)_3$, under air their emission quantum efficiency is ~21% and 82% of that of $Ir(ppy)_3$, due to their insensitivity toward air. This insensitivity may be attributed to the short decay lifetime of the Pt(II) complexes. At 77 K, in frozen CH_2Cl_2, complexes **1a** and **2a** also display phosphorescence (see Table 1 and SI).

Interactions with Zn(II) Ions. In addition to forming Pt(II) complexes, the new ligands are also capable of binding to Zn(II) ions, which can be monitored readily by UV−vis, fluorescence, and NMR spectra. Because of the intense current interest in Zn(II) ion sensing,[14] we decided to examine the interaction of $Zn(ClO_4)_2$ with our four new ligands in THF.

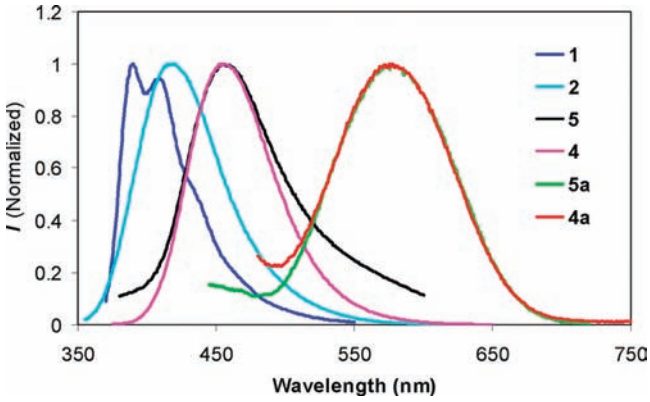

Figure 6. Emission spectra of the free ligands **1**, **2**, **4**, and **5** and complexes **4a** and **5a** in THF (1.0×10^{-5} M) at ambient temperature.

As shown in Figure 7, the binding of the three 4,4′-functionalized bpy ligands to a Zn(II) ion generates a distinct spectral change. For both **4** and **5**, the λ_{max} of the low-energy absorption band is red-shifted by 40−60 nm upon Zn(II) binding, resulting in a change of the solution color from colorless to yellow. A similar absorption spectral red shift has been observed in 4,4′-aminoaryl-functionalized

(14) (a) Bozym, R. A.; Thompson, R. B.; Stoddard, A. K.; Fierke, C. A. *Chem. Biol.* **2006**, *1*, 103. (b) Kimura, E.; Kikuta, E. *J. Biol. Inorg. Chem.* **2000**, *5*, 139. (c) Nolan, E. M.; Jaworski, J.; Okamoto, K.-I.; Hayachi, Y.; Sheng, M.; Lippard, S. J. *J. Am. Chem. Soc.* **2005**, *127*, 16812. (d) Jamieson, E. R.; Lippard, S. J. *Chem. Rev.* **1999**, *99*, 2467. (e) Hang, L.; Murphy, C. S.; Kuang, G. C.; Hazelwood, K. L.; Constantino, M. H.; Davidson, M. W.; Zhu, L. *Chem. Commun.* **2009**, 7408. (f) Hang, L.; Clark, R. J.; Zhu, L. *Chem.—Eur. J.* **2008**, *14*, 2894.

(15) Sénéchal, K.; Maury, O.; Le Bozec, H. Ledoux, I.; Zyss, J. *J. Am. Chem. Soc.* **2002**, *124*, 4560, and references therein.

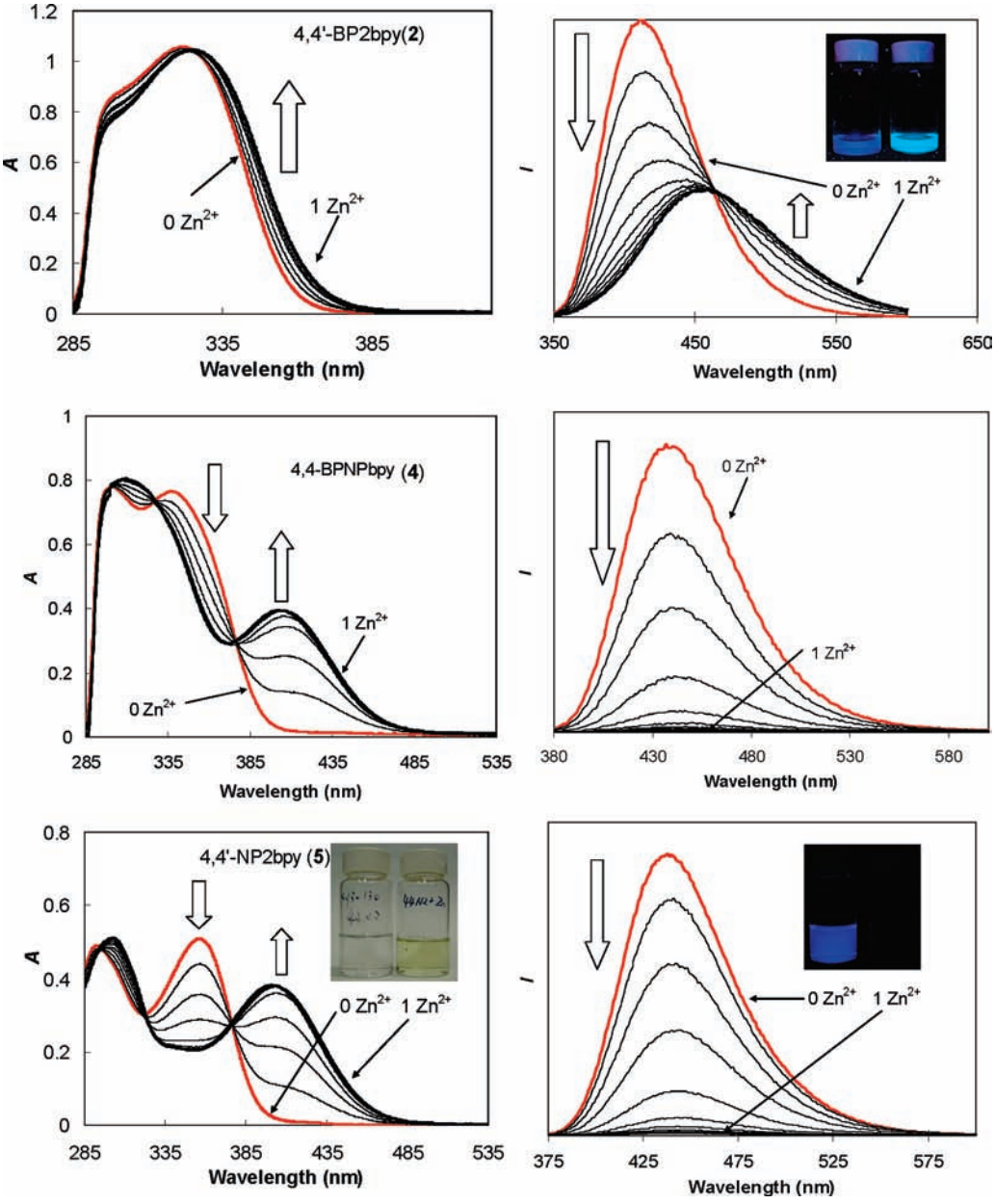

Figure 7. UV−vis (right) and fluorescence (left) spectral change of ligands 4,4′-BP2bpy (**2**), 4,4′-BPNPbpy (**4**), and 4,4′-NP2bpy (**5**) with the addition of $Zn(ClO_4)_2$ in THF (~1.0×10^{-5} M).

2,2′-bpy Zn(II) complexes and attributed to an intraligand charge-transfer transition.[15] The emission spectra of **4** and **5** are quenched by Zn(II) ions. The response of **2** toward Zn(II) ions is unique among the 4,4′-functionalized ligands: its absorption spectrum only experiences a ~5 nm red shift, while its emission spectrum has a ~40 nm red shift with a distinct emission color change from deep blue to sky blue, as shown in Figure 7. The lack of an amino donor group in **2** is clearly responsible for its distinct fluorescence "turn-on" response to Zn(II) ions, although the details are been understood.

The absorption spectral change of **1** with Zn(II) ions is similar to that of **2** with Zn(II) ions (see SI). However, the emission spectrum of **1** undergoes a complete quenching in the same manner as that of **4** and **5**, thus demonstrating that the fluorescence response of the bpy derivative ligands toward Zn(II) can be greatly influenced by not only the nature of the substituent group but also the geometry of the ligand. Stern−Volmer plots (see SI) indicate that the Zn(II) ion forms a 1:2 complex with the bpy derivative ligands ($[ZnL_2]^{2+}$), which is also supported by NMR and MS spectral data for the isolated compound $[Zn(4,4'\text{-BP2bpy})](ClO_4)_2$. Using the absorption spectral titration data, the overall binding constants of ligands **1**, **2**, **4**, and **5** with Zn(II) ions were estimated by using a general fitting equation.[16] The results of the fitting support that the Zn(II) ion indeed forms a 1:2 complex with the bpy ligands. The overall binding constant K was found to be similar for all boryl ligands (1.2×10^{11} M^{-2}

(16) (a) Connors, K. A. *Binding Constants*; John Wiley and Sons: New York, 1987. (b) Valeur, B. *Molecular Fluorescence: Principles and Applications*; Wiley-VCH: Weinheim, 2002. (c) Peng, X.; Du, J.; Fan, J.; Wang, J.; Wu, Y.; Zhao, J.; Sun, S.; Xu, T. *J. Am. Chem. Soc.* **2007**, *129*, 1500.

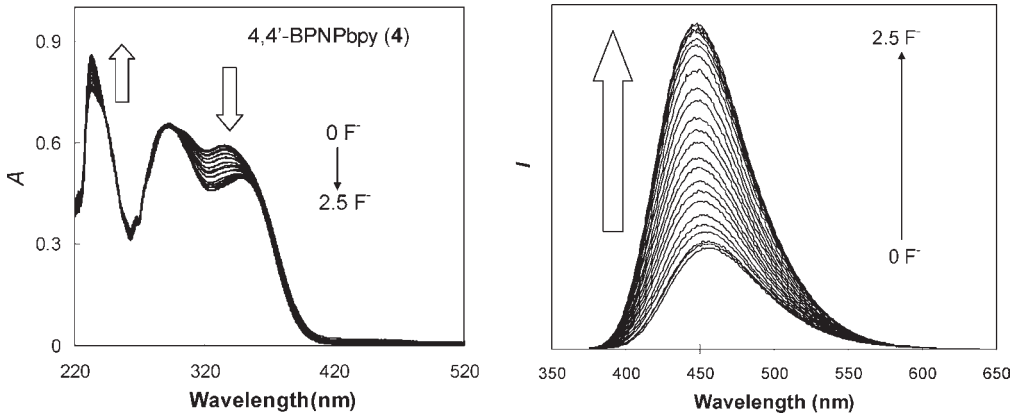

Figure 8. UV−vis (left) and fluorescence (right) spectral change of 4,4′-BPNPbpy (**4**) (~1.0×10^{-5} M) with the addition of NBu_4F (λ_{ex} = 350 nm) in CH_2Cl_2 (~1.0×10^{-5} M).

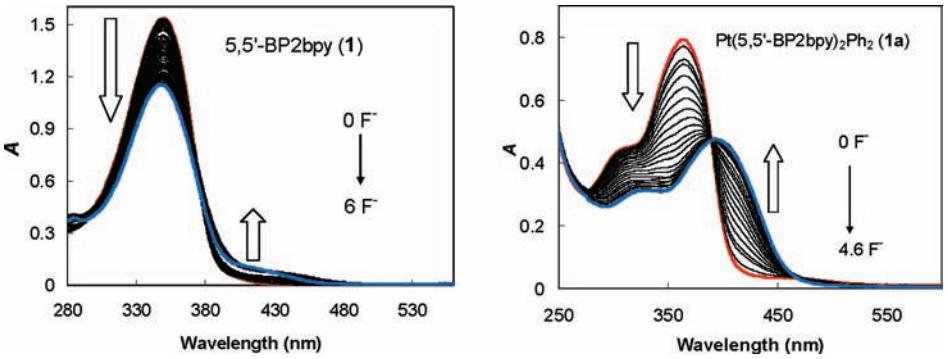

Figure 9. Absorption spectral change of 5,5′-BP2bpy (**1**) and its Pt(II) complex Pt(5,5′-BP2bpy)$_2$Ph$_2$ (**1a**) with the addition of NBu_4F in CH_2Cl_2 (~1.0×10^{-5} M).

for **1**, 2.7×10^{11} M^{-2} for **2** and **4**). The donor-only ligand **5** was found to have a greater binding strength toward Zn(II), compared to the boryl ligands, with $K = 7.8 \times 10^{11}$ M^{-2}. For details, please see section S8 in the SI. The magnitude of these binding constants is consistent with those reported previously for Zn(II) complexes with bpy derivative ligands.[14]

Response to Fluorides and Cyanides. The Zn(II) complexes are unstable toward fluorides, which causes the dissociation of the bpy derivative ligand from the Zn(II) center. Our study has therefore focused on the interaction of the boron-containing free ligands **1**, **2**, and **4** and the corresponding Pt(II) complexes with fluoride ions.

For diboryl compound **1**, the addition of $[NBu_4]F$ causes an intensity decrease of the intense absorption band at 350 nm and the appearance of a weak shoulder band at ~430 nm. For **2**, the absorption band at 322 nm is quenched and blue-shifted (see SI). Unlike 5,5′-B2bpy, which shows a distinct stepwise formation of the 1:1 and 1:2 fluoride adducts,[6a,b] **1** and **2** do not show a stepwise addition of fluoride ions, an indication of a much diminished electronic communication between the two boron centers in **1** and **2** due to the much longer linker group. For both molecules, the emission band is completely quenched by the addition of the fluoride ions (see SI). In contrast, for the donor−acceptor molecule **4**, the addition of F^- causes a substantial intensity increase of the emission peak with a ~10 nm blue shift (from 457 to 447 nm) and a small intensity decrease of the low-energy absorption band (Figure 8). This "turn-on" response toward fluoride is reminiscent of that of 4,4′-BNbpy we reported recently[6b] and can be attributed to the switching from a charge-transfer transition of the ligand to a $\pi \rightarrow \pi^*$ transition and the relative high emission quantum efficiency of the fluoride adduct. The difference is that the emission peak of 4,4′-BNbpy experiences a much greater blue shift (~100 nm) than that of **4** upon binding with fluoride ions, thus resulting in a distinct color change from blue-green to deep blue, which can be attributed to the much shorter conjugated linker in 4,4′-BNbpy, compared to that in **4**. Efforts to obtain the stepwise binding constants (K_1 and K_2) for the two diboryl molecules **1** and **2** with fluoride ions were unsuccessful due to the lack of a distinct stepwise change of the titration spectra. Nonetheless, we were able to obtain the overall binding constant K for these two molecules using fluorescence titration data.[16] The magnitude of the overall binding constants (~2×10^8 M^{-2} for **1** and ~6×10^8 M^{-2} for **2**, ~2×10^5 M^{-1} for **4** ($K = K_1$)) indicates that the binding strength of these new boron compounds with fluoride ions is similar to that of typical triarylboron compounds $B(Mes)_2(Ar)$,[4] but much less than that of 5,5′-B2bpy, where the two $B(Mes)_2$ groups are directly attached to the bpy ring.[6a,b]

For complex **1a**, the addition of fluoride ions causes the decrease of the absorption band at 369 nm and the appearance of a new band at 395 nm, a behavior similar to that of the free ligand, as shown in Figure 9, and attributable to the narrowing of the $\pi-\pi^*$ gap caused by the switching of two electron-withdrawing $BMes_2$ groups

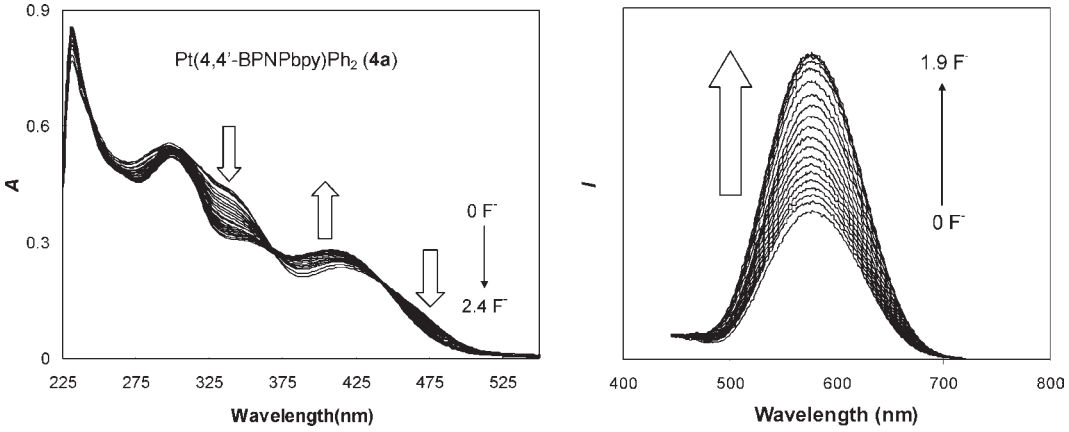

Figure 10. UV−vis (left) and emission (right) spectral change of Pt(4,4′-BPNPbpy)$_2$Ph$_2$ (**4a**) with the addition of NBu$_4$F in CH$_2$Cl$_2$.

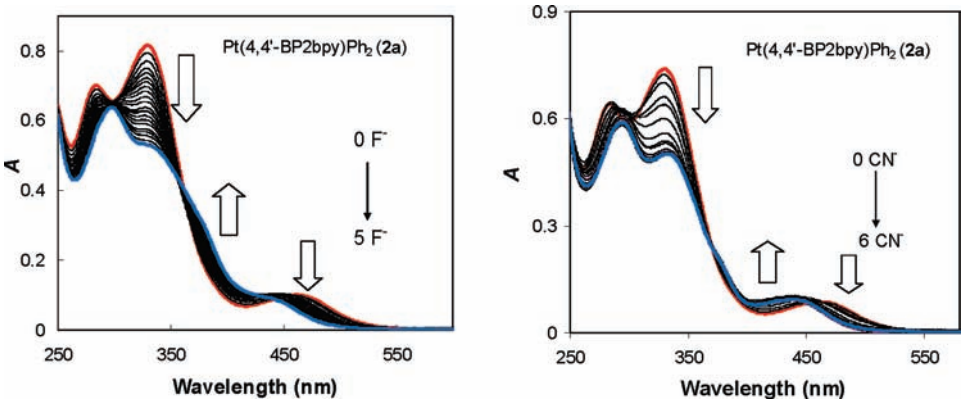

Figure 11. UV−vis spectral change of Pt(4,4′-BP2bpy)$_2$Ph$_2$ (**2a**) with the addition of NBu$_4$F (left) and NBu$_4$CN (right) in CH$_2$Cl$_2$.

to electron-donating BMes$_2$(F) groups. In contrast to Pt(5,5′-B2bpy)Ph$_2$, which has a distinct MLCT color change from red to orange, then to light yellow with the sequential addition of one and two equivalents of fluoride ions,[6a] **1a** does not have such a distinct color change due to the lack of a strong and distinct MLCT band.

For complexes **2a** (Figures 10 and 11) and **4a**, the MLCT absorption band is quenched by fluorides with a blue shift of the spectrum. The emission spectrum of **4a** experiences a dramatic increase in intensity in the same manner as that of the free ligand (Figures 8 and 10), further supporting that the origin of the emission is ligand-centered. In addition, the Pt(II) complexes have consistently a stronger binding with the fluoride ion, compared to the free ligand, as shown by the Stern−Volmer plots (see SI). Using the absorption titration data, the overall binding constants for the Pt(II) complexes were estimated[16] to be $\sim 2 \times 10^9$ M^{-2} for **1a**, $\sim 7 \times 10^8$ M^{-2} for **2a**, and $\sim 6 \times 10^5$ M^{-1} for **4a**.

Interestingly, the boron center in the Pt(II) complexes is also capable of binding to CN^- without the dissociation of the bpy ligand. The spectral change with the cyanide addition resembles that of fluoride addition, as shown by the UV−vis titration diagrams of **2a** by F^- and CN^-, in Figure 11. The overall binding constant K ($\sim 2 \times 10^9$ M^{-2}) for the CN^- binding was found to be similar to that of F^- binding with **2a** (see SI). Using triarylboron-functionalized metal complexes to detect CN^- anions has been demonstrated recently.[3−5]

Conclusions

Two diboryl molecules, one donor−acceptor molecule and one donor-only molecules based on either a 5,5′-biphenyl-2,2′-bpy or a 4,4′-biphenyl-2,2′-bpy core, have been achieved. Compared to 5,5′-B2bpy, which contains the 2,2′-bpy core only, extending the π-conjugation via the phenyl ring, in general, diminishes the electronic communication between the two boron centers and their electron-accepting ability/Lewis acidity, although it does significantly enhance the emission quantum efficiency of the 5,5′-diboryl molecule **1**. The molecular geometry has been found to have a significant impact on the properties of the molecule, as illustrated by the much lower quantum efficiency of the 4,4′-diboryl-substituted molecule **2**, compared to **1**, and the fact that molecule **1** is a "turn-off" fluorescence sensor while **2** is a "turn-on" sensor for Zn(II) ions. Extending the π-conjugation of the bpy-based ligands also significantly blue-shifts the energy of the MLCT band of the Pt(II) complex of the 5,5′-diboryl molecule **1**, causing the loss of a dramatic visual color change upon binding with fluoride that is characteristic of the Pt(II) complexes of 5,5′-B2bpy. Extending the π-conjugation does not change the fluorescence/phosphorescence "turn-on" response of the donor−acceptor molecule **4** and its Pt(II) complex toward fluoride, but does cause the loss of a distinct emission color change, compared to 5,5′-BNbpy and its Pt(II) complex. Finally, cyanide ions can bind to the boron center of the PtPh$_2$

complexes based on the boryl-functionalized 2,2′-bpy ligands in the same manner as fluoride ions without disrupting the Pt−bpy chelate bonds. Using the new ligands in the synthesis of polyboryl transition metal complexes such as Ru(II) is in progress, and the results will be reported in due course.

Acknowledgment. We thank the Natural Sciences and Engineering Research Council of Canada for financial support.

Supporting Information Available: This material is available free of charge via the Internet at http://pubs.acs.org.